Computational Methods in Water Resources 2022

Three-dimensional Rayleigh-Darcy convection at high Rayleigh numbers

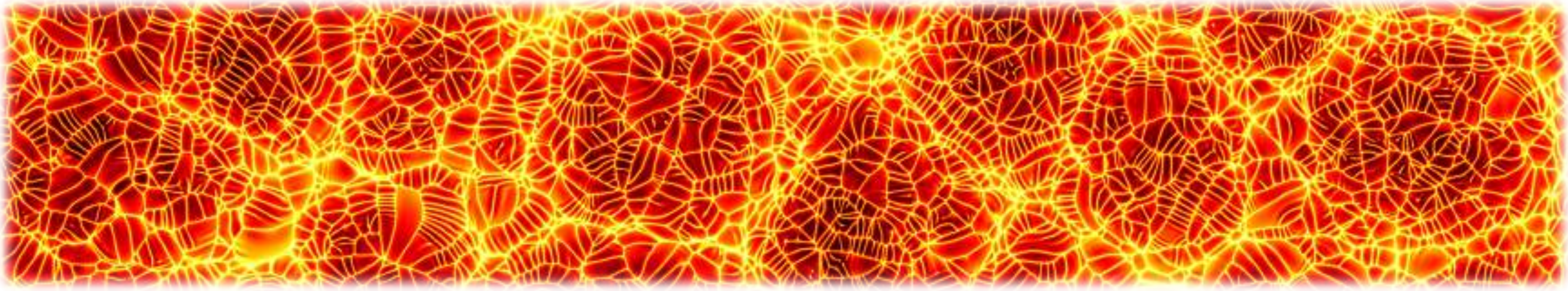

Physics of Fluids

M. De Paoli[1,2], F. Zonta[2], S.Pirozzoli[3] & A. Soldati[2,4]

[1]Physics of Fluids Group, University of Twente, Enschede (The Netherlands)
[2]Institute of Fluid Mechanics and Heat Transfer, TU Wien, Vienna (Austria)
[3]Department of Aerospace and Mechanical Engineering, La Sapienza University, Rome, (Italy)
[4]Polytechnic Department, University of Udine, Udine (Italy)

TU WIEN

UNIVERSITAS · STUDIORUM · UTINENSIS

SAPIENZA
UNIVERSITÀ DI ROMA

m.depaoli@utwente.nl
https://marcodepaoli.com

CMWR 2022

June 19-23, 2022, Gdansk (Poland) (hybrid)

Carbon Capture and Storage

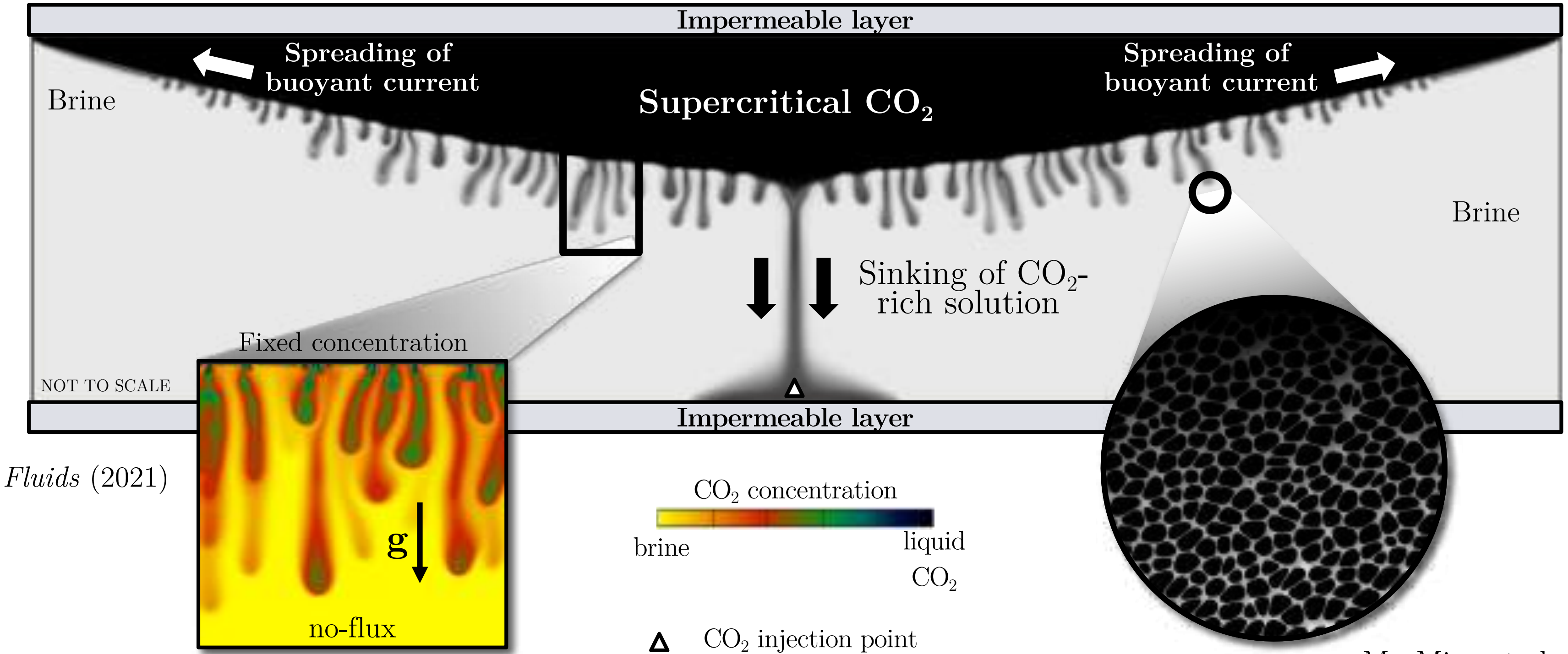

De Paoli, *Phys. Fluids* (2021)

MacMinn et al., *Geophys. Res. Lett.* (2013)

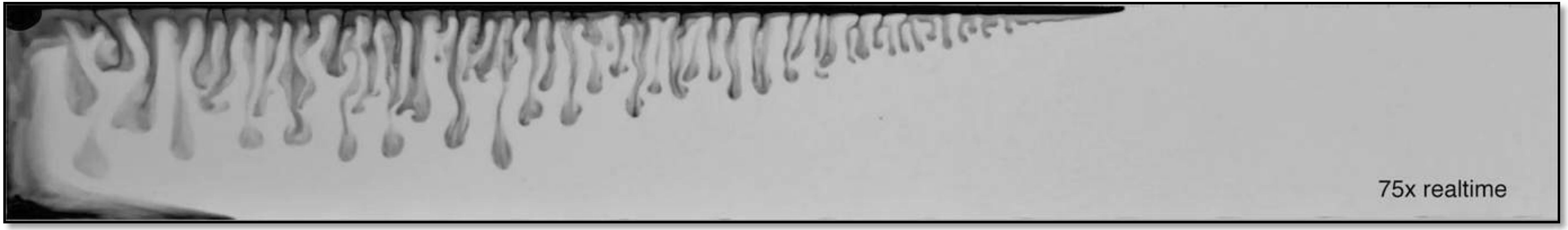

Methodology

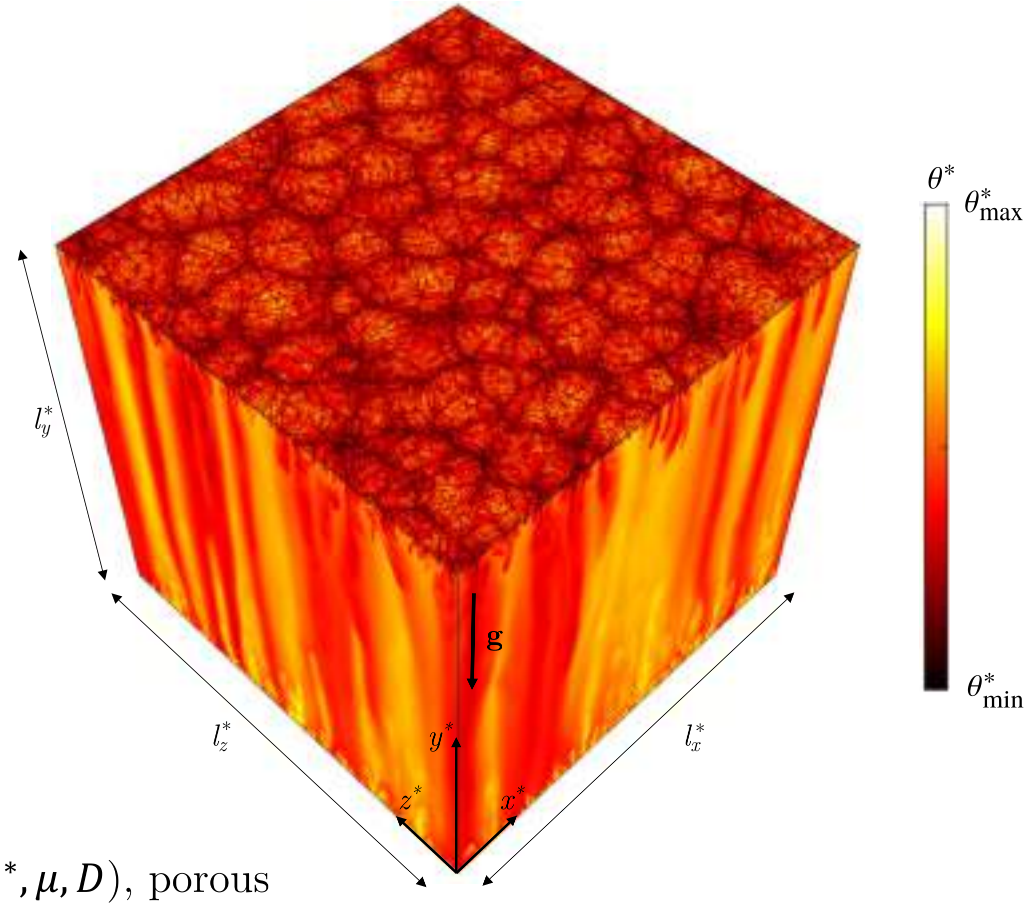

Fluid $(\Delta\rho^*, \mu, D)$, porous medium (κ, ϕ) and domain (l_y^*) properties → $Ra = g\Delta\rho^*\kappa l_y^*/(\phi D\mu)$

De Paoli, Pirozzoli, Zonta & Soldati, *J. Fluid Mech.* (in press)
Pirozzoli, De Paoli, Zonta & Soldati, *J. Fluid Mech.* (2021)

Equations

$$\frac{\partial\theta}{\partial t} + \nabla\cdot\left(\mathbf{u}\theta - \frac{1}{\mathrm{Ra}}\nabla\theta\right) = 0,$$

$$\nabla\cdot\mathbf{u} = 0 \quad , \quad \mathbf{u} = -\left(\nabla p - \theta\mathbf{j}\right),$$

Boundary conditions

$$v(y=0) = 0 \quad , \quad \theta(y=0) = 1,$$
$$v(y=1) = 0 \quad , \quad \theta(y=1) = 0.$$

Simulations performed

Simulation	Ra	$l_x/l_y \times l_z/l_y$	$N_x \times N_z \times N_y$
Ra_1	1.0×10^3	4×4	$384\times384\times32$
Ra_2	2.5×10^3	4×4	$768\times768\times64$
Ra_5	5.0×10^3	4×4	$1536\times1536\times128$
Ra_7	7.5×10^3	4×4	$2304\times2304\times192$
Ra_{10}	1×10^4	1×1	$768\times768\times256$
Ra_{20}	2×10^4	1×1	$1536\times1536\times512$
Ra_{30}	3×10^4	1×1	$2304\times2304\times768$
Ra_{40}	4×10^4	1×1	$3072\times3072\times1024$
Ra_{80}	8×10^4	1×1	$6144\times6144\times2048$

Numerical details

- Spatial discretization: Second-order finite-difference incompressible flow solver (staggered arrangement of the flow variables, Orlandi, *Fluid Flow Phenomena*, 2000)
- Time discretization: the temperature transport equation is advanced in time by means of a hybrid third-order low-storage Runge–Kutta algorithm, whereby the convective terms are handled explicitly and the diffusive terms are handled implicitly, limited to the wall-normal direction.
- Pure MPI parallelization: Cineca Supercomputing centre, Infrastructure Marconi,

32,000 cores
$\approx$ 3TB/field

Equations

$$\frac{\partial \theta}{\partial t} + \nabla \cdot \left(\mathbf{u}\theta - \frac{1}{\mathrm{Ra}} \nabla \theta \right) = 0,$$

$$\nabla \cdot \mathbf{u} = 0 \quad , \quad \mathbf{u} = -\left(\nabla p - \theta \mathbf{j} \right),$$

Boundary conditions

$$v(y=0) = 0 \quad , \quad \theta(y=0) = 1,$$
$$v(y=1) = 0 \quad , \quad \theta(y=1) = 0.$$

Simulations performed

Simulation	Ra	$l_x/l_y \times l_z/l_y$	$N_x \times N_z \times N_y$
Ra_1	1.0×10^3	4×4	$384 \times 384 \times 32$
Ra_2	2.5×10^3	4×4	$768 \times 768 \times 64$
Ra_5	5.0×10^3	4×4	$1536 \times 1536 \times 128$
Ra_7	7.5×10^3	4×4	$2304 \times 2304 \times 192$
Ra_{10}	1×10^4	1×1	$768 \times 768 \times 256$
Ra_{20}	2×10^4	1×1	$1536 \times 1536 \times 512$
Ra_{30}	3×10^4	1×1	$2304 \times 2304 \times 768$
Ra_{40}	4×10^4	1×1	$3072 \times 3072 \times 1024$
Ra_{80}	8×10^4	1×1	$6144 \times 6144 \times 2048$

De Paoli, Pirozzoli, Zonta & Soldati, *J. Fluid Mech.* (in press)
Pirozzoli, De Paoli, Zonta & Soldati, *J. Fluid Mech.* (2021)

Temperature and heat transfer statistics

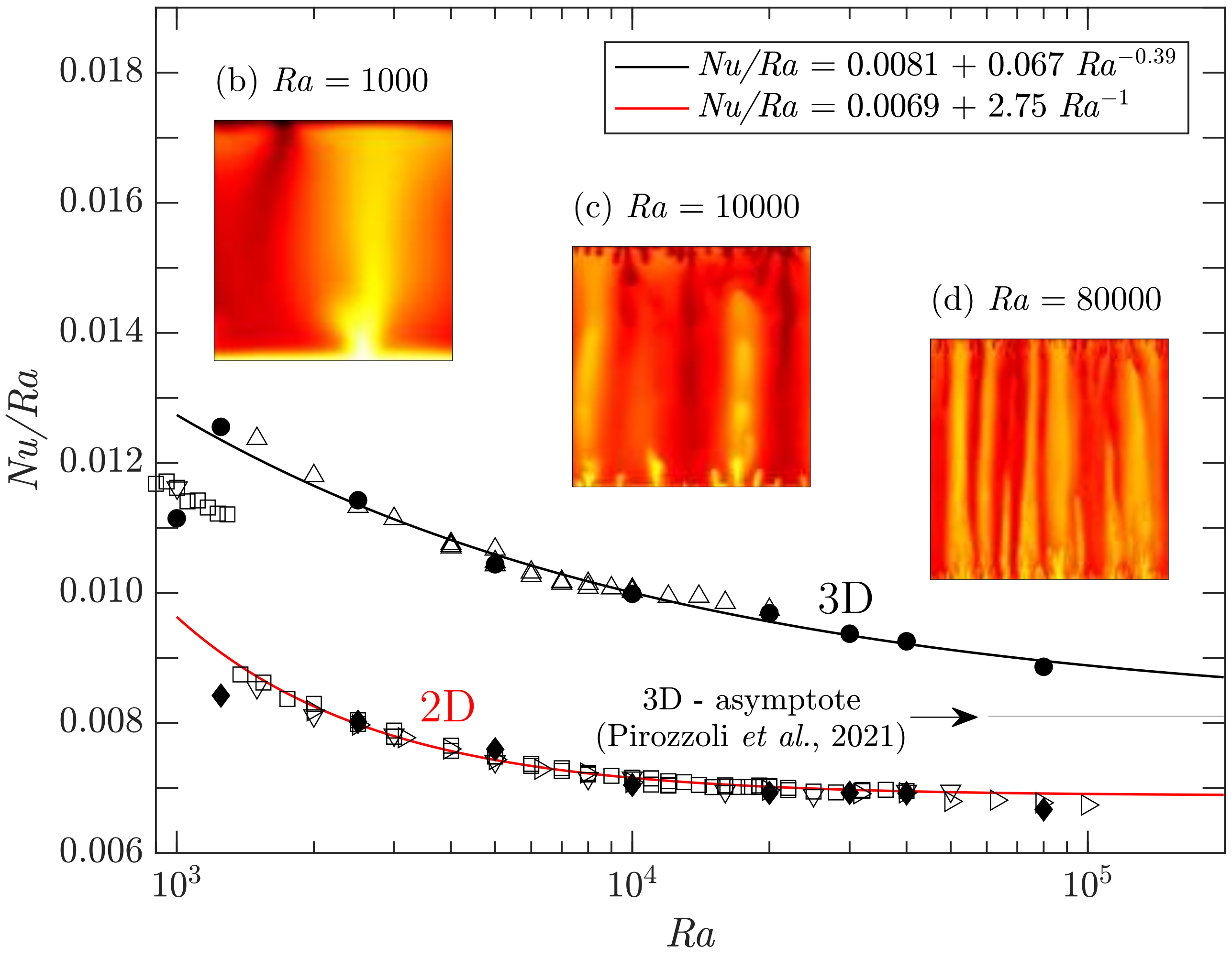

filled symbols: Pirozzoli *et al.* (2021),
open symbols: Hewitt *et al.* (2012,2014), Wen *et al.* (2015)

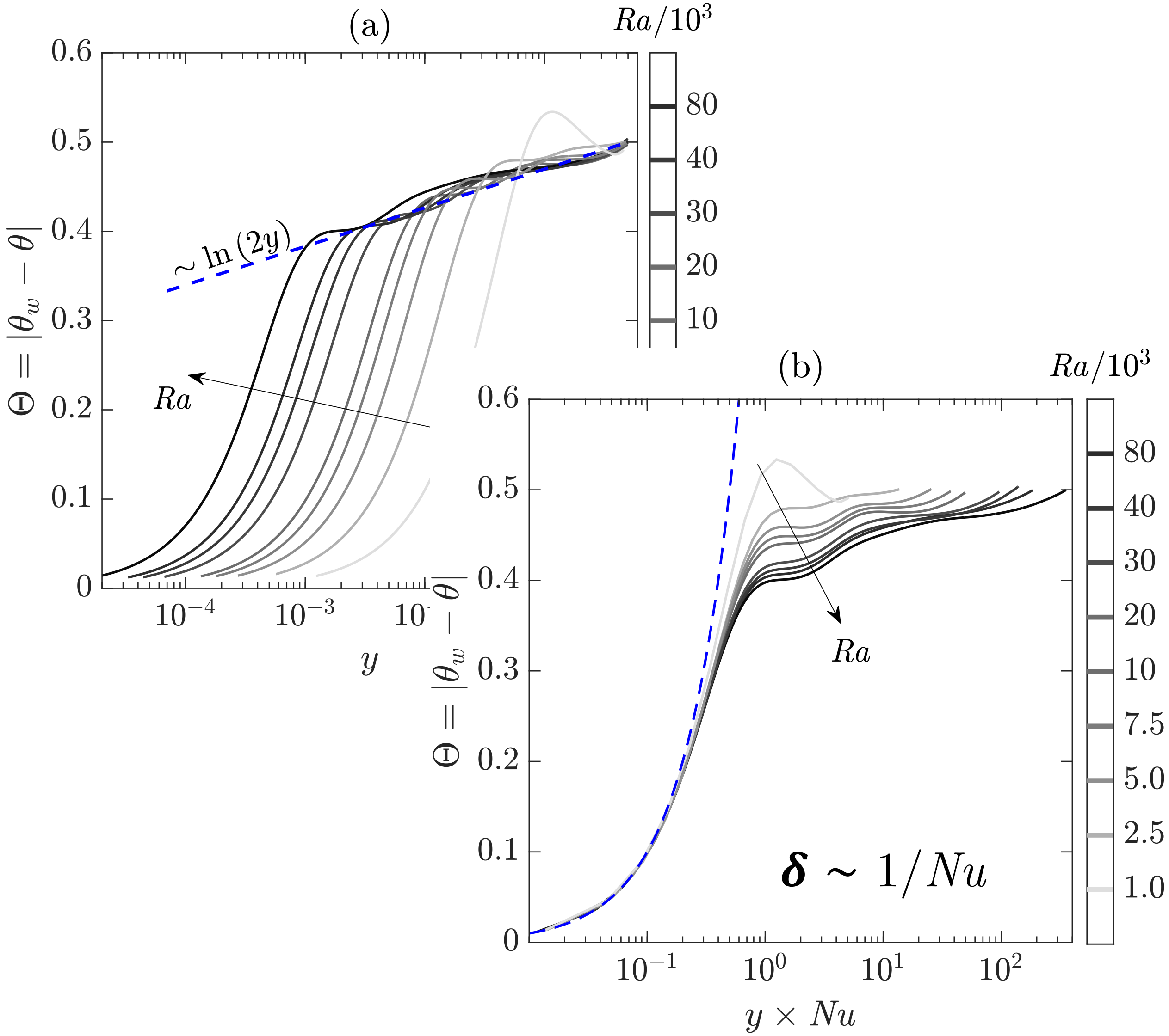

Physics of Fluids

Flow structure at high-Ra ($Ra = 8 \times 10^4$)

y-z slice ($x = 0$)

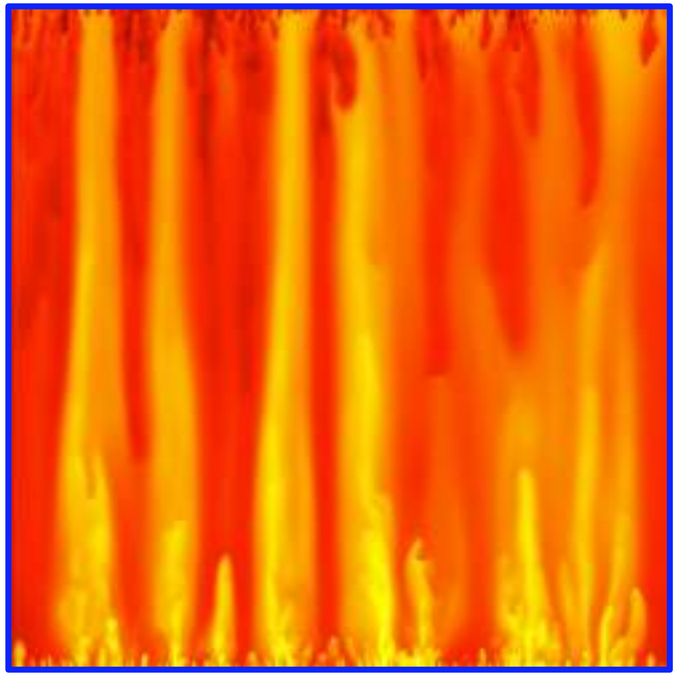

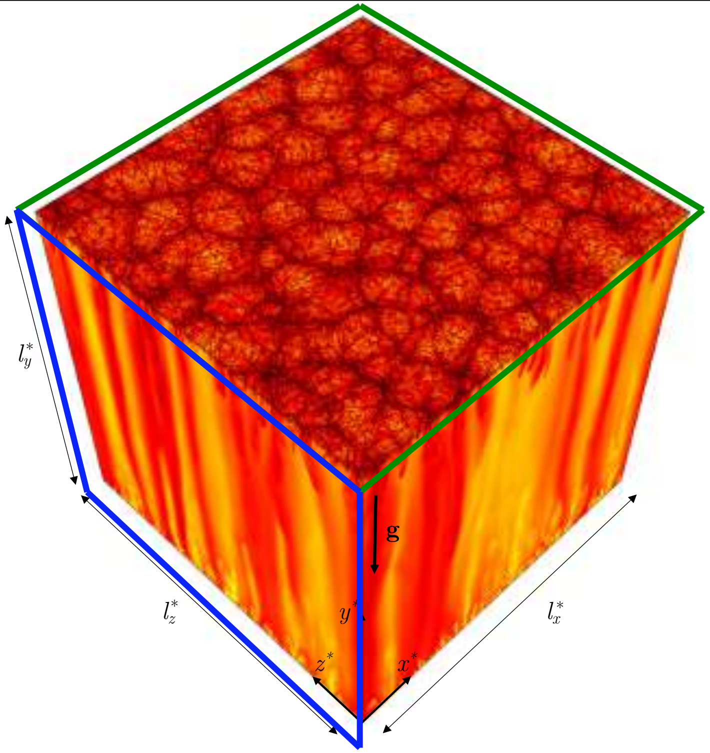

x-z slice ($y = 0.01$)

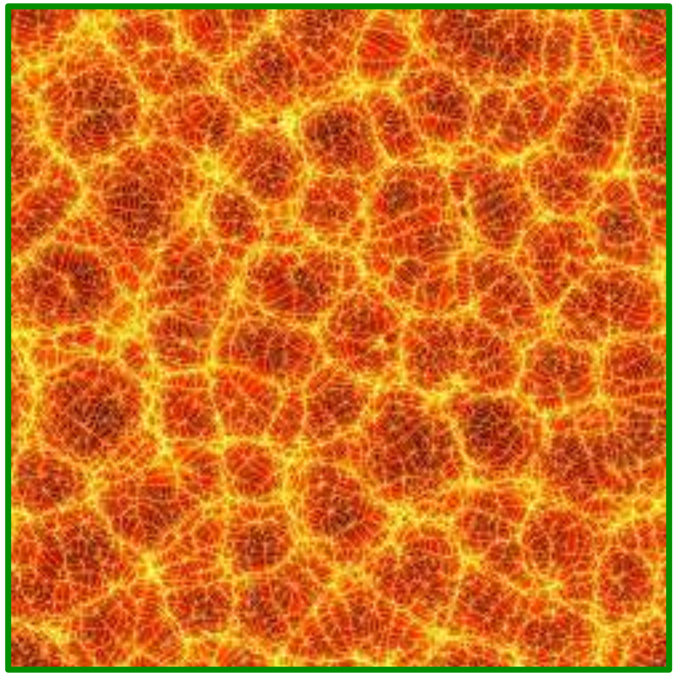

Pirozzoli, De Paoli, Zonta & Soldati, *J. Fluid Mech* (2021)

Characterization of near-wall cell pattern

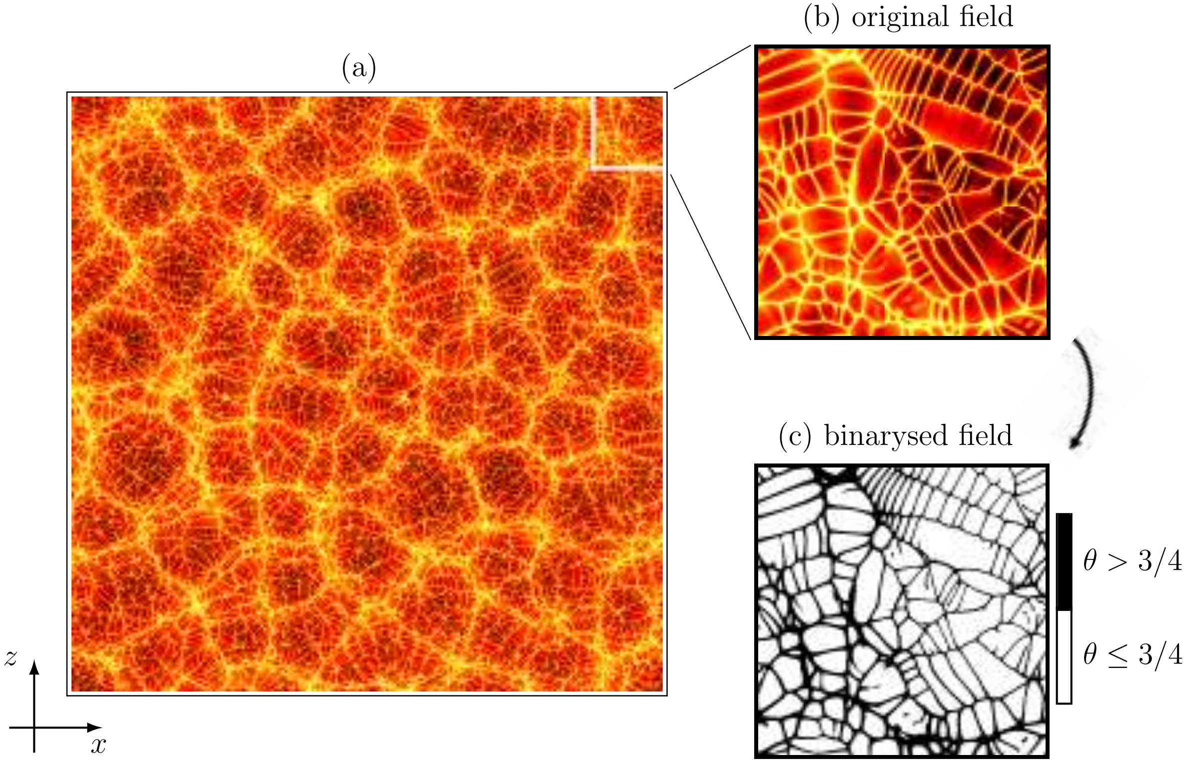

Near-wall temperature field binarization

Characterization of cell pattern:

- Identification of cells area, A
- Identification of cells shape (circularity, C)

$\mathcal{C} = 4\pi A/\Pi^2$, with Π the cell perimeter.

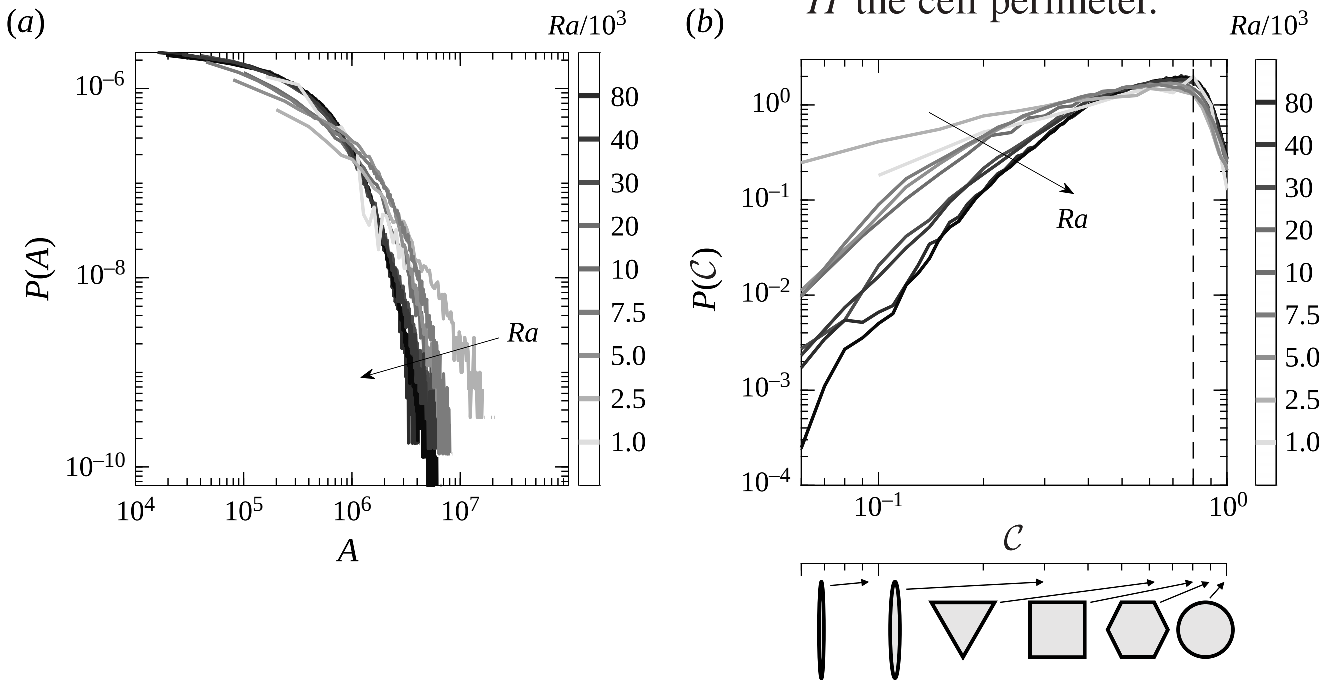

De Paoli, Pirozzoli, Zonta & Soldati, *J. Fluid Mech.* (in press)

Near-wall and core flow

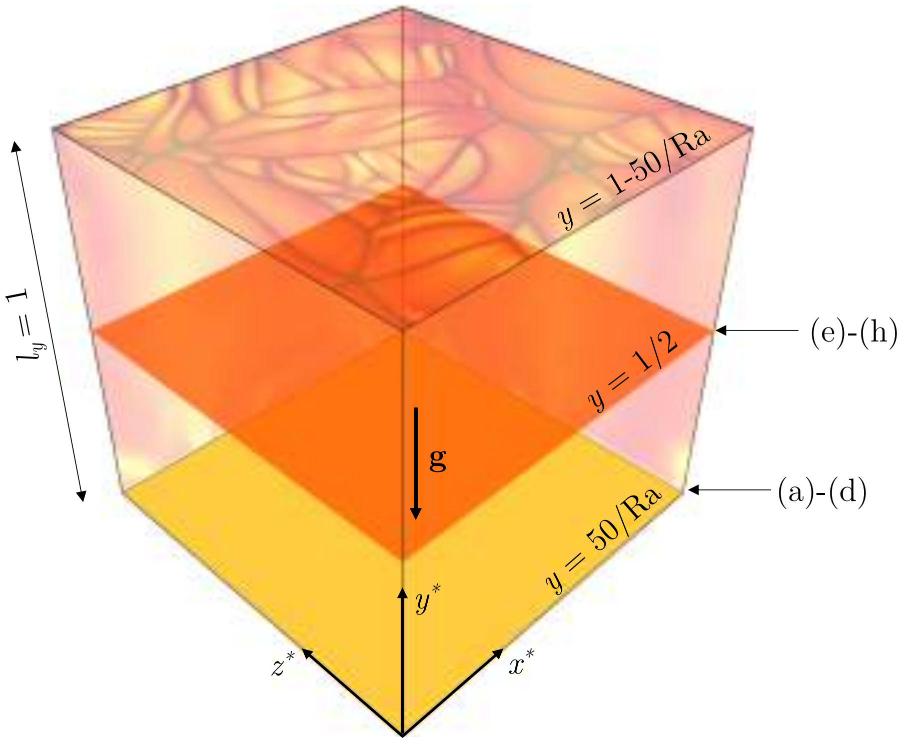

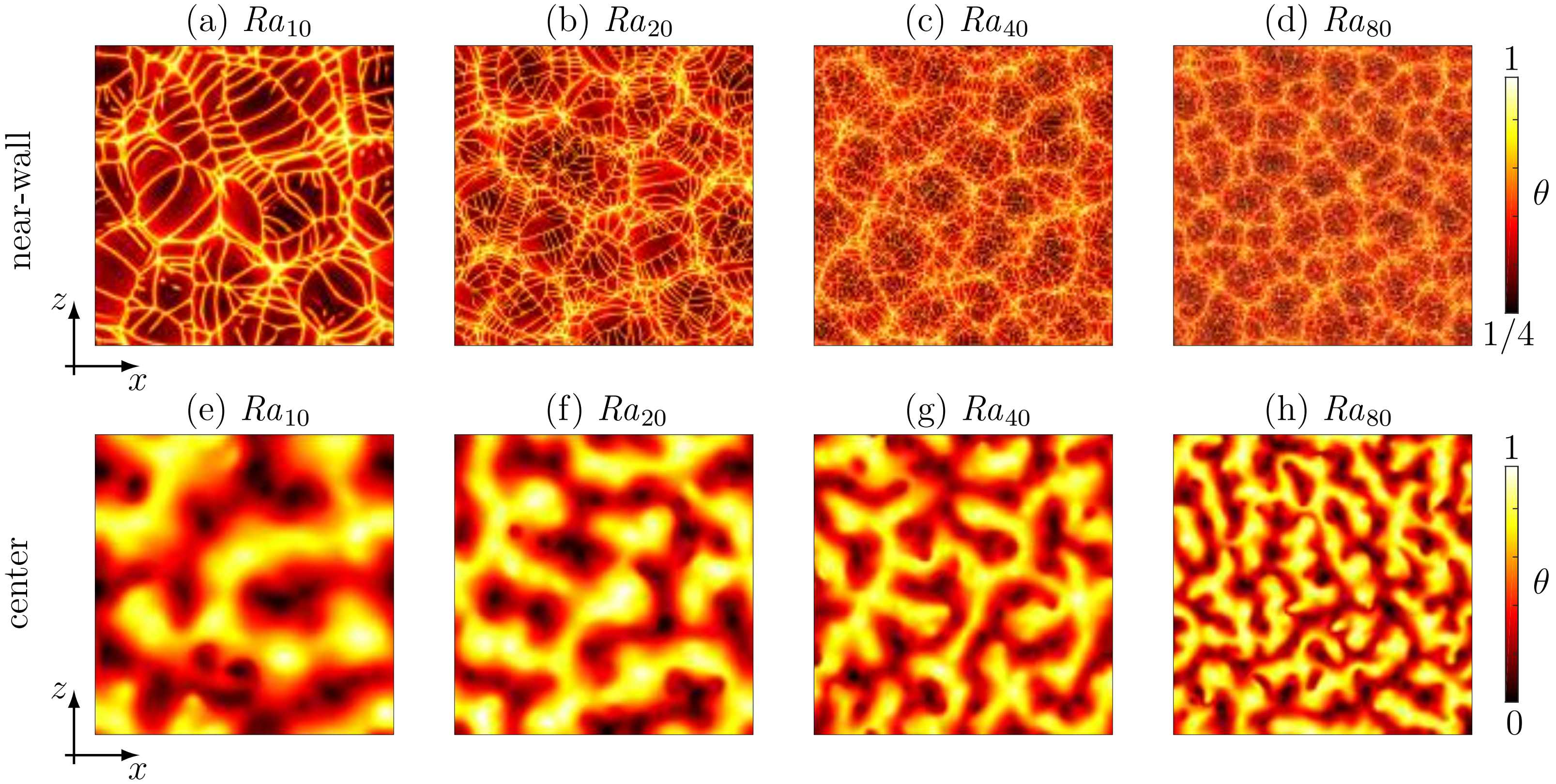

Are supercells correlated to megaplumes?

Near-wall flow structures and supercells

$Ra = 80{,}000$, horizontal slice near the wall

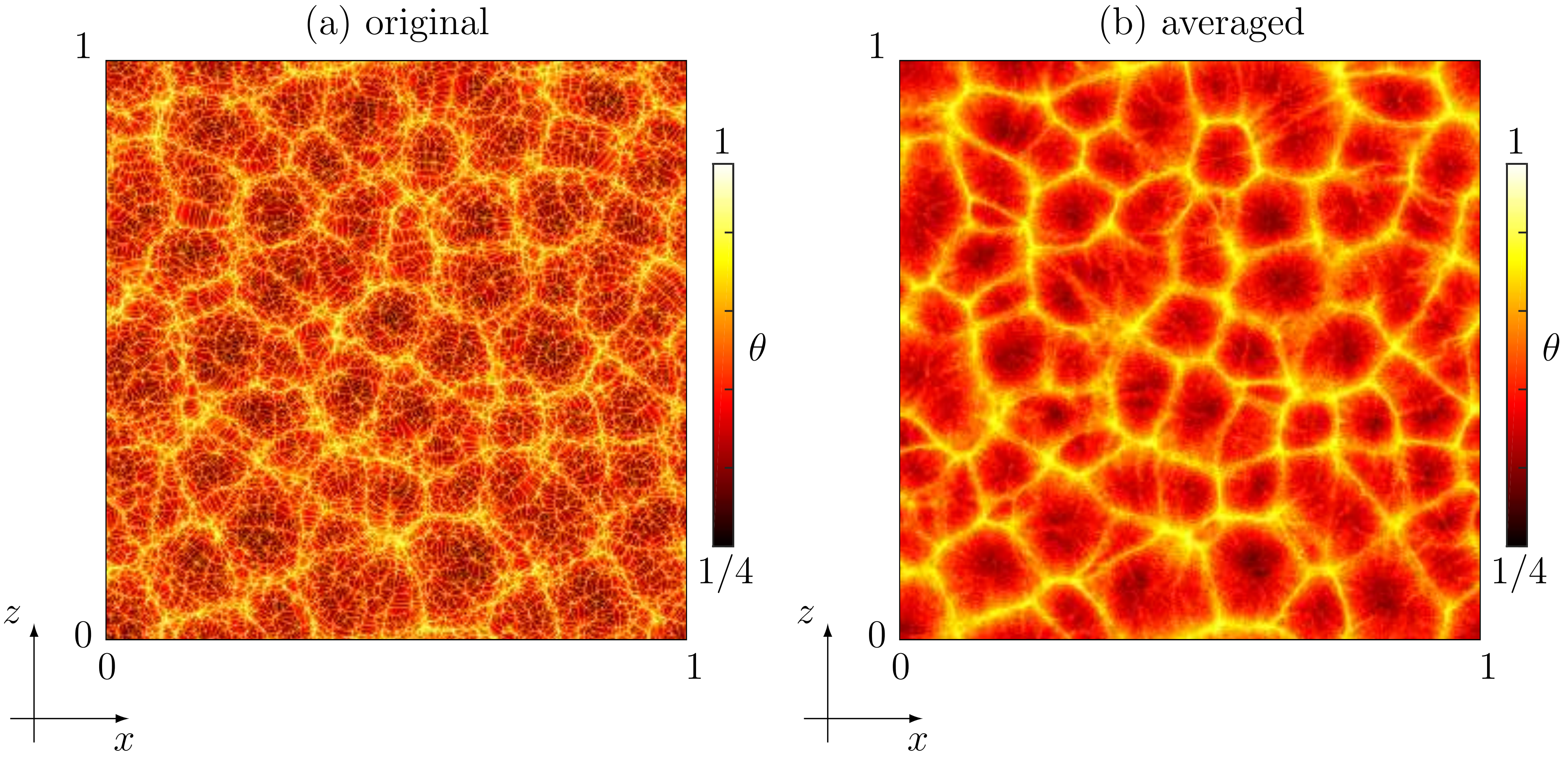

Mean radial wave number

$$\overline{k}_r(y) = \left\langle \frac{\int\int \sqrt{k_x^2 + k_z^2}\, E(k_x, k_z)\, \mathrm{d}x\mathrm{d}z}{\int\int E(k_x, k_z)\, \mathrm{d}x\mathrm{d}z} \right\rangle$$

Theoretical prediction (Hewitt *et al.*, 2014):

center

$$\overline{k}_r \sim Ra^{1/2}$$

near-wall

$$\overline{k}_r \sim \boldsymbol{\delta} \sim 1/Nu$$

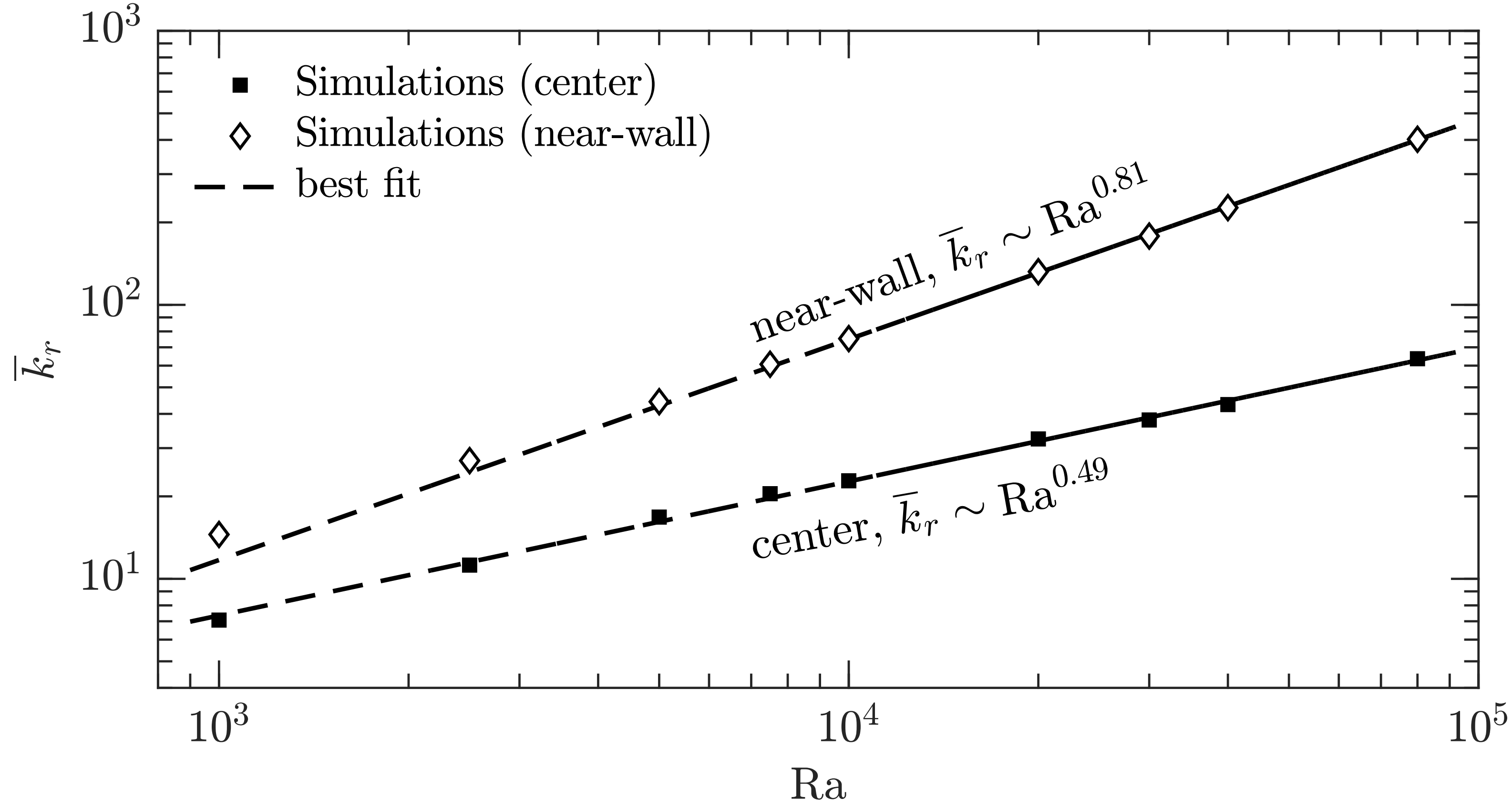

Supercells and megaplumes

Mean radial wave number

$$\overline{k}_r(y) = \left\langle \frac{\int\int \sqrt{k_x^2 + k_z^2}\, E(k_x, k_z)\, \mathrm{d}x\mathrm{d}z}{\int\int E(k_x, k_z)\, \mathrm{d}x\mathrm{d}z} \right\rangle$$

Following Berghout *et al.* (2021), we filter out the small-scale structures

Supercells are the footprint of megaplumes

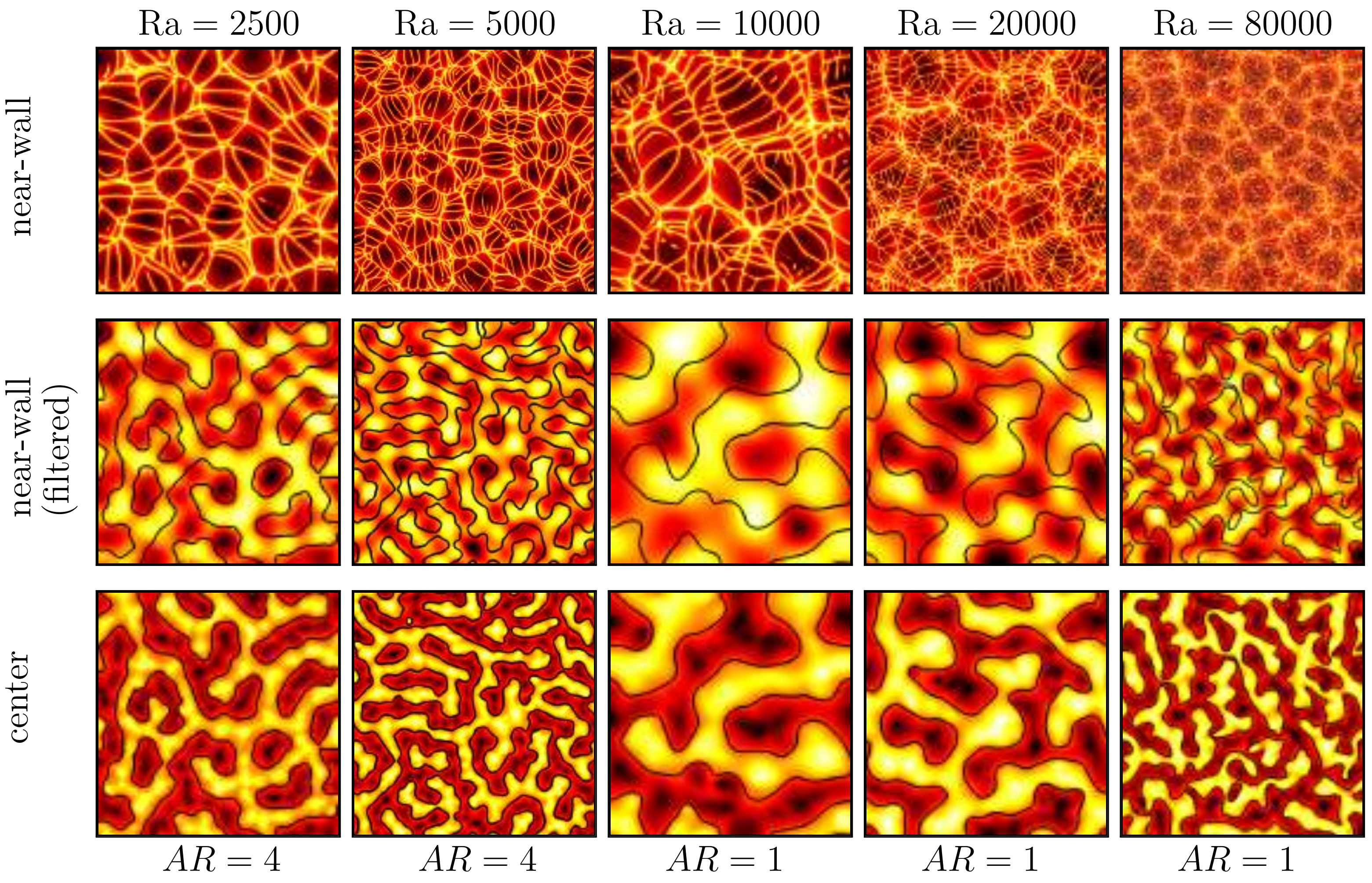

Mean radial wave number

$$\overline{k}_r(y) = \left\langle \frac{\int\int \sqrt{k_x^2 + k_z^2}\, E(k_x, k_z)\, \mathrm{d}x\mathrm{d}z}{\int\int E(k_x, k_z)\, \mathrm{d}x\mathrm{d}z} \right\rangle$$

Following Berghout *et al.* (2021), we filter out the small-scale structures

$$r = \left\langle \frac{\int\int (\theta - \overline{\theta}_f)(\theta_f - \overline{\theta}_f)\, \mathrm{d}x\, \mathrm{d}z}{\sqrt{\int\int (\theta - \overline{\theta}_f)^2 \mathrm{d}x\, \mathrm{d}z}\sqrt{\int\int (\theta_f - \overline{\theta}_f)^2 \mathrm{d}x\, \mathrm{d}z}} \right\rangle$$

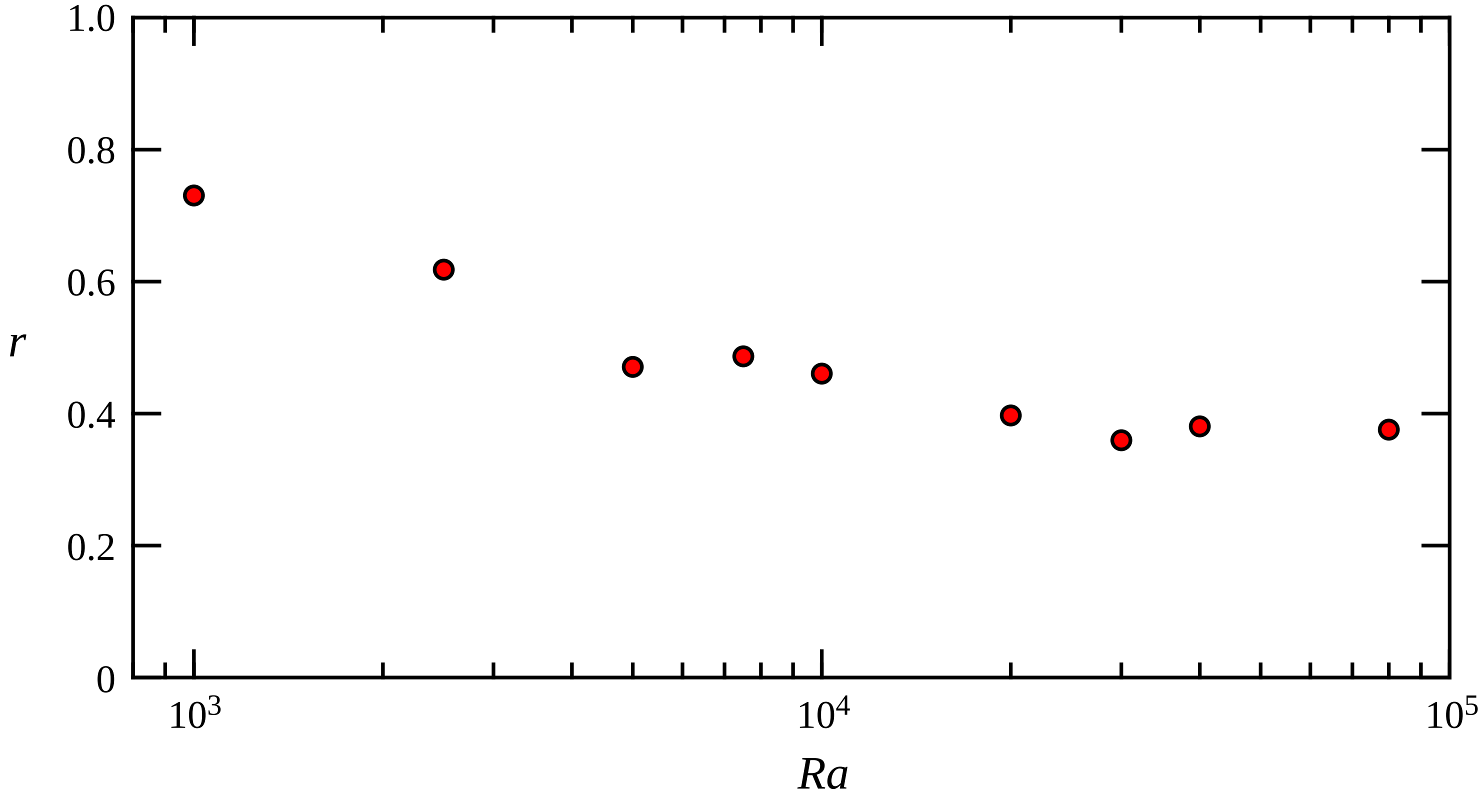

Supercells are the footprint of megaplumes

Assessment of domain size effects

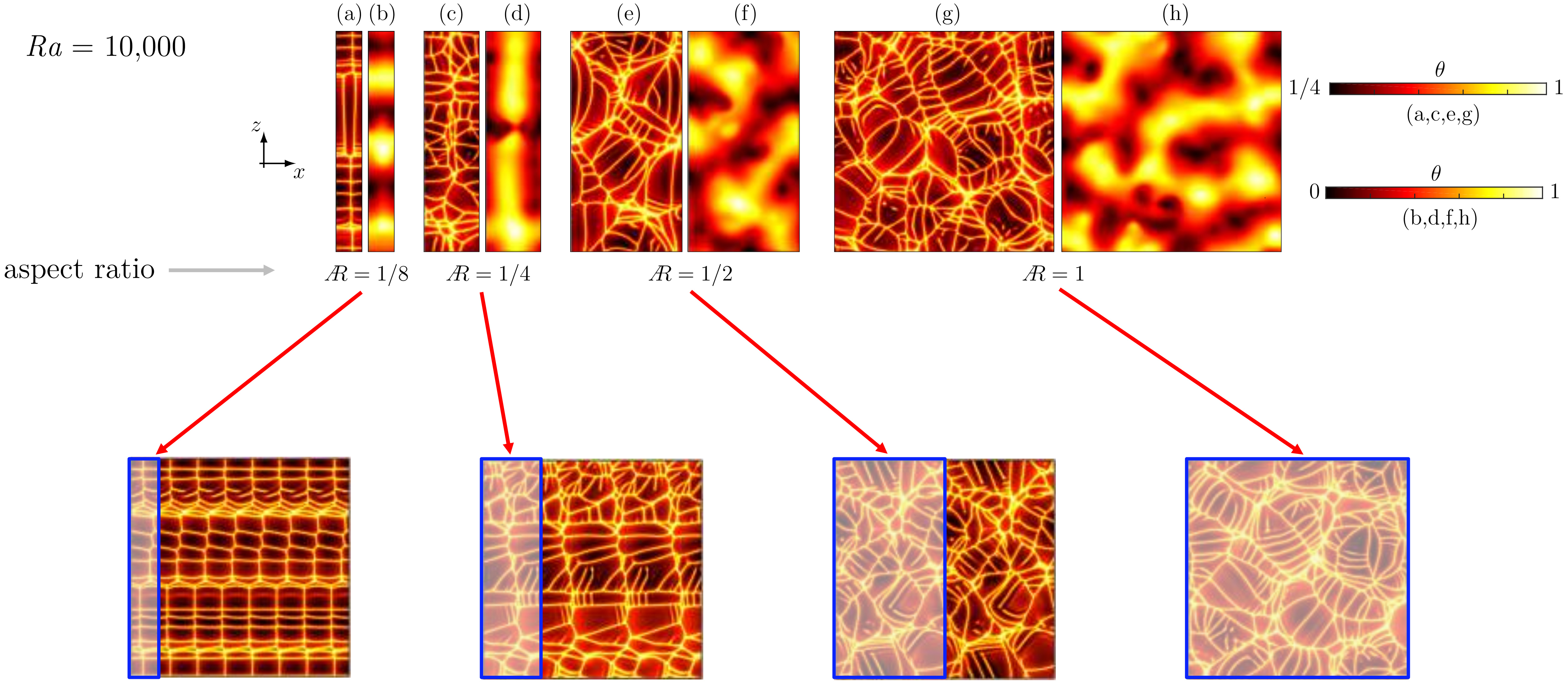

Assessment of domain size effects

$Ra = 10{,}000$

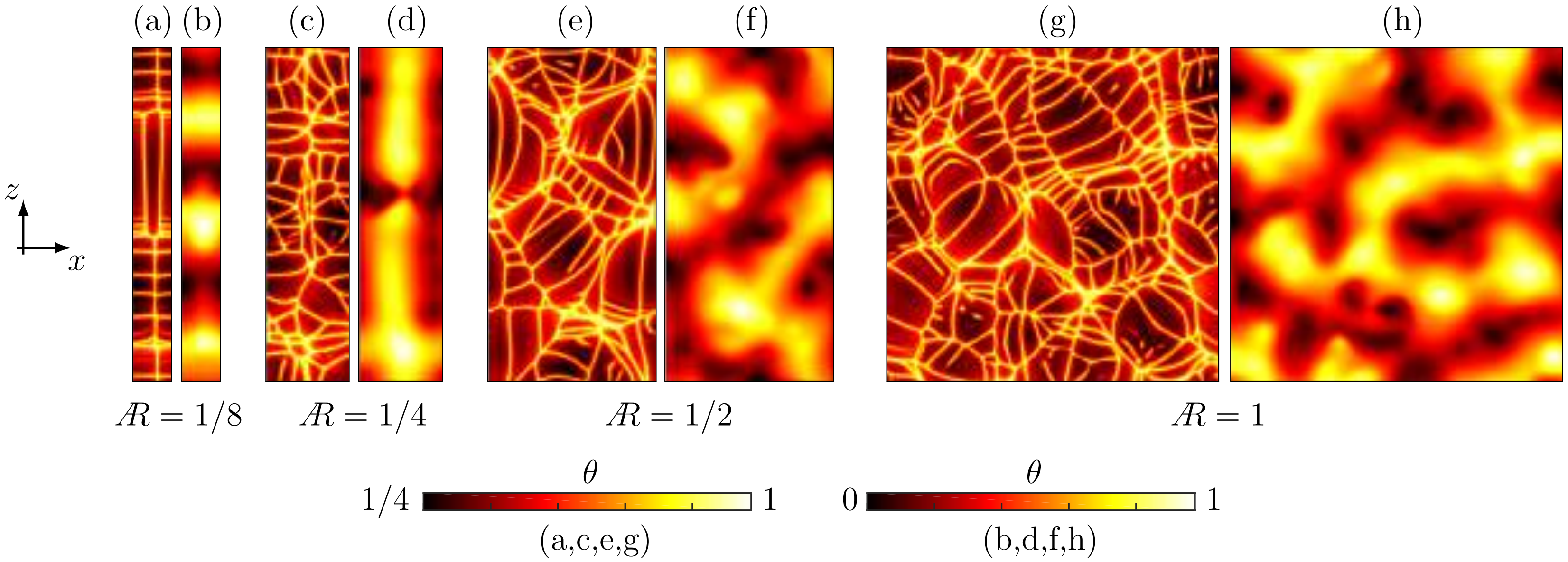

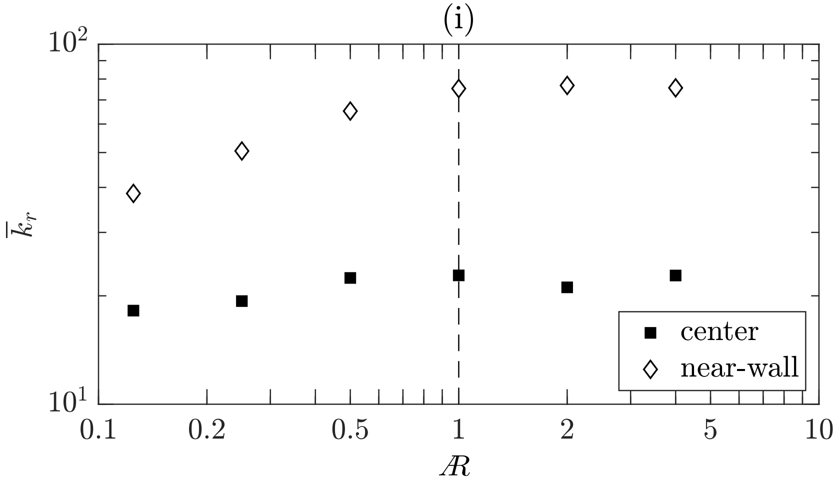

Also at large Ra [$O(10^3)$], a minimum aspect ratio of 1 is required to accurately describe the large-scale flow structures

Future developments – pore-scale dynamics

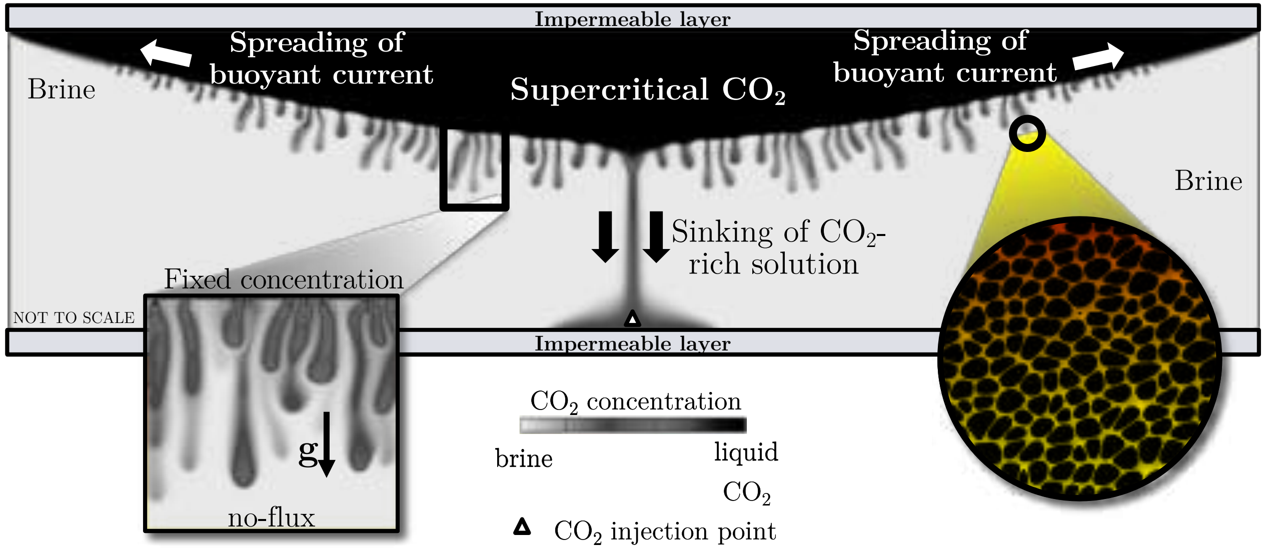

Numerical and experimental investigation of pore-scale dispersion effects on convective dissolution

Experiment (beads 4 mm)

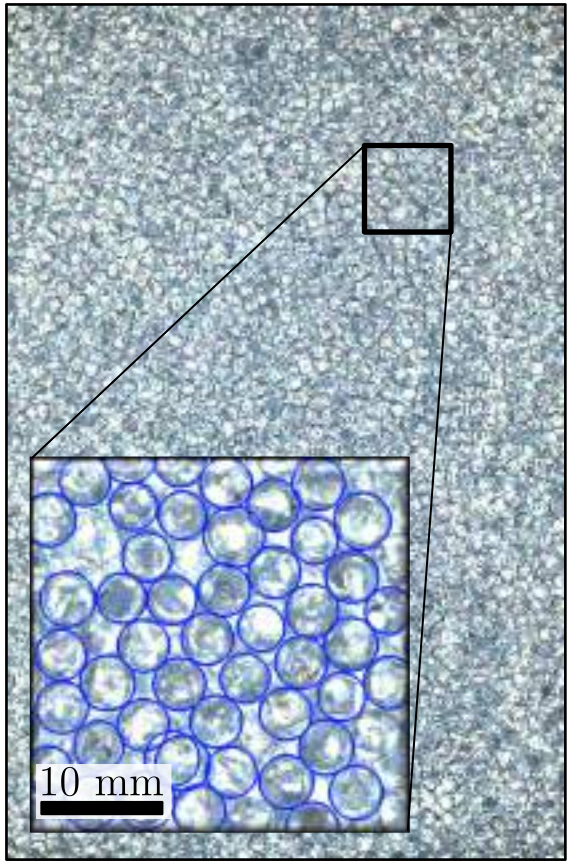

Simulations (IBM)

Chris Howland, *Physics of Fluids Group*, University of Twente

Thank you for your attention!
Questions?

This research was funded in part by the Austrian Science Fund (FWF) [Grant J-4612]

Der Wissenschaftsfonds.

HPC resources provided by PRACE [Grant Pra21-5415]

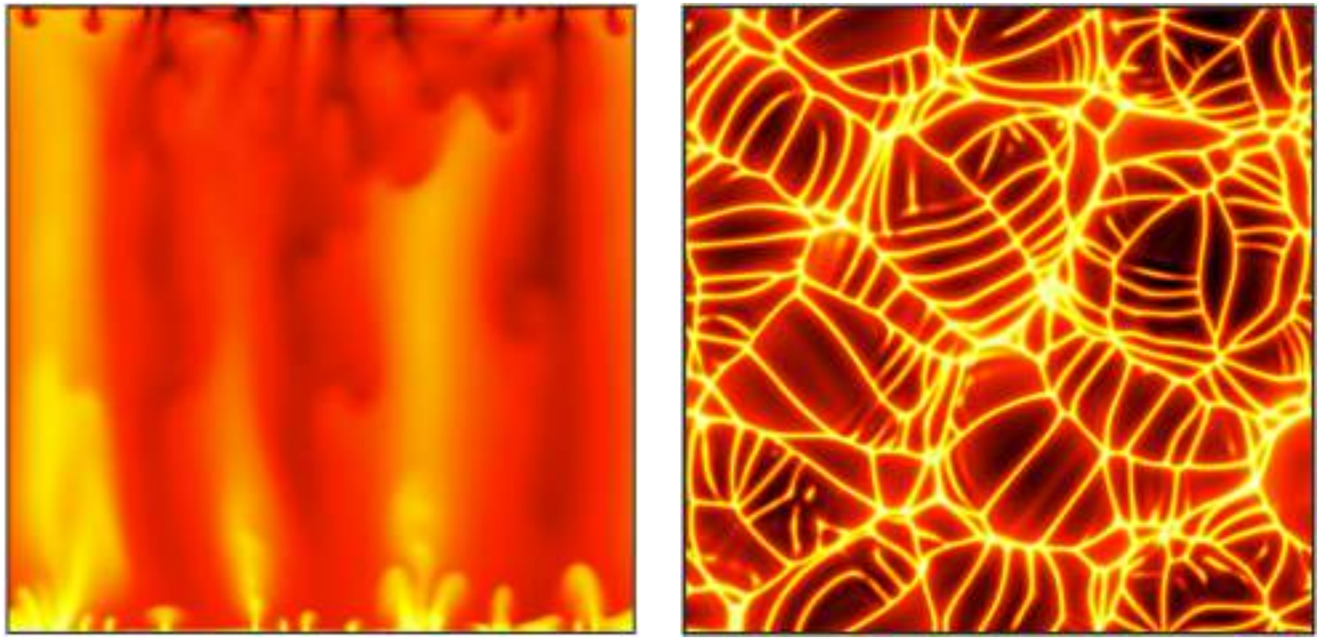

Physics Today **74**, 5, 68 (2021)

Additional numerical details

Additional details on spatial discretization

- Wall-normal direction: hyperbolic tangent stretching function
  - Approximately 20 points within the thermal boundary layer
- Horizontal directions: uniform spacing
- Fourier expansion along the horizontal periodic directions yields a system of tridiagonal equations in the wall-normal direction for each Fourier mode, which is then solved with standard highly efficient numerical techniques

Equations

$$\frac{\partial \theta}{\partial t} + \nabla \cdot \left(\mathbf{u}\theta - \frac{1}{\mathrm{Ra}} \nabla \theta \right) = 0,$$

$$\nabla \cdot \mathbf{u} = 0 \quad , \quad \mathbf{u} = -\left(\nabla p - \theta \mathbf{j} \right),$$

Boundary conditions

$$v(y=0) = 0 \quad , \quad \theta(y=0) = 1,$$
$$v(y=1) = 0 \quad , \quad \theta(y=1) = 0.$$

The pressure field is determined by solving the Poisson equation resulting from the divergence-free constraint:

$$\nabla^2 p = \frac{\partial \theta}{\partial y}$$

$\partial p / \partial y = 0$ at walls (no-penetration)

De Paoli, Pirozzoli, Zonta & Soldati, *J. Fluid Mech.* (in press)
Pirozzoli, De Paoli, Zonta & Soldati, *J. Fluid Mech.* (2021)

High-resolution images, movies and slides are available upon request to m.depaoli@utwente.nl